

Modeling force-induced bio-polymer unfolding

Anthony J. Guttmann¹, Jesper L. Jacobsen², Iwan Jensen¹ and Sanjay Kumar³

¹ ARC Centre of Excellence for Mathematics and Statistics of Complex Systems,

Department of Mathematics and Statistics,

The University of Melbourne, Victoria 3010, Australia

² Université Paris Sud, UMR8626, LPTMS, F-91405 Orsay Cedex, France

Service de Physique Théorique, CEA Saclay, F-91191 Gif-sur-Yvette, France

³Department of Physics, Banaras Hindu University, Varanasi 221 005, India

October 25, 2018

Abstract

We study the conformations of polymer chains in a poor solvent, with and without bending rigidity, by means of a simple statistical mechanics model. This model can be exactly solved for chains of length up to $N = 55$ using exact enumeration techniques. We analyze in details the differences between the constant force and constant distance ensembles for large but finite N . At low temperatures, and in the constant force ensemble, the force-extension curve shows multiple plateaus (intermediate states), in contrast with the abrupt transition to an extended state prevailing in the $N \rightarrow \infty$ limit. In the constant distance ensemble, the same curve provides a unified response to pulling and compressing forces, and agrees qualitatively with recent experimental results. We identify a cross-over length, proportional to N , below which the critical force of unfolding decreases with temperature, while above, it increases with temperature. Finally, the force-extension curve for stiff chains exhibits “saw-tooth” like behavior, as observed in protein unfolding experiments.

Keywords: Protein unfolding, Polymers, Lattice models, Exact enumerations

1 Introduction

In order to understand the role of molecular interactions in the structural behaviour of bio-molecules, it has been found appropriate to introduce force as a thermodynamic variable [1, 2]. This development, which has occurred only in the last decade, permits the experimental study of a variety of properties of bio-molecules, including elastic, functional, mechanical and structural properties [3]. Furthermore, the variation of force with other parameters, such as solvent pH, loading rate and temperature helps us understand the interactions better [4, 5, 6]. Many biological reactions involve large conformational changes, with well defined responses. For example, the radius of gyration of a polymer may display substantial variation, and this can be used to follow the reaction as it progresses [3].

In these cases, a conceptually simple two-state model can be used to track the process [3]. The applied force twists the free energy surface along the reaction co-ordinate by an amount proportional to the radius of gyration. There are several important transitions of this type, including the folding-unfolding transition [1], the stretching and unzipping of dsDNA [7, 8], and the ball-string polymer transition [9]. Away from the θ -temperature, we know that a polymer will be in either a collapsed or a swollen state [10]. The mean-square radius of gyration $\langle R^2 \rangle_g$ scales with chain length N as $\langle R^2 \rangle_g \sim \text{const.} \times N^{2\nu}$, where ν is the critical exponent. At low temperatures, when the polymer is in the collapsed state, $\nu = 1/d$ while at high temperature $\nu = 1, 3/4, 0.588\dots, 1/2$ for $d = 1, 2, 3, 4$ [10] respectively. These values are believed to be exact for $d = 1, 2$ and, with a logarithmic correction, for $d = 4$. For $d = 3$ the (approximate) numerical estimate is obtained from a variety of series expansion, Monte Carlo and field theory methods, which are all in agreement within error bars. It should be noted that a polymer cannot acquire the conformation of a fully stretched state (characterised by $\nu = 1$), by varying the temperature alone. Application of sufficient force will achieve this stretched state. Hence it can be seen that force not only twists the free energy surface, but also introduces a new stretched state, which is not otherwise accessible. Furthermore, recent experiments [9, 11, 12] suggest that there are a number of intermediate states achieved as the polymer is unfolded, which manifest themselves as a sequence of plateaus in the force-scaled elongation plots.

In studying such problems, there are two relevant ensembles. These are the *constant force ensemble* (**CFE**) and the *constant distance ensemble* (**CDE**). The former ensemble has predominantly been used in the study of the non-equilibrium thermodynamics of small systems, where the average extension is taken as the control parameter. In atomic force microscopy, the force is usually applied using a linear ramp protocol with very small velocity, so changes take place extremely slowly. In such cases the **CDE** is the appropriate ensemble. While one might expect the choice of ensemble to be irrelevant in the thermodynamic limit [13], for small systems, such as single molecules, the results are expected to be ensemble dependent [14]. Other aspects of the experimental situation that have been largely ignored include the loss of entropy due to the effective confinement induced by such features as the attachment of receptor and ligand molecules to a substrate and a transducer, respectively.

These transitions have typically been studied using very simple models, such as the freely-jointed chain (FJC) or the worm-like chain (WLC) [15, 16]. These models ignore important effects such as excluded volume, and attractive interactions, and though they have been used to study the force-extension curves of bio-molecules [16], they are really only suited to do so in a good solvent. In a poor solvent, as mentioned above, the force-extension curves display plateaus at certain values of force [9, 11]. A combination of an improved theoretical understanding of semi-flexible polymers, combined with new experimental observations of polymers in poor solvents have given rise to improved levels of understanding of globules with a well defined internal structure [17, 18]. These developments, in turn, have potential application to the study and understanding of the basic mechanism of protein folding.

In this paper we provide several results. Firstly a complete phase diagram based on an analysis of exact enumerations of finite chains of unprecedented lengths. We particularly focus our attention on the low-temperature regime, for it is this region that is so difficult to access either experimentally, or by other theoretical techniques, such as Monte Carlo methods. These studies are very relevant to certain features of single bio-molecules that are studied experimentally. In particular, we find intermediate low-temperature states stabilised by the force. We also find that there is a cross-over length, below which the transition temperature is a decreasing function of force, while above it

increases with force.

We also introduce, for the first time, a bending rigidity, and repeat our calculations with an additional parameter that tunes for stiffness. For appropriate high values of bending rigidity, we find saw-tooth like oscillations. These have been observed experimentally, but as far as we are aware, have not been previously modelled.

A brief account of our work has appeared recently [19]. The present paper provides a more detailed discussion and several new results.

In the next section we define our model precisely, and in section 3 we calculate fluctuations in the number of contacts as a function of force for fixed temperature, and vice versa. We use the positions of the peaks in the fluctuation curves as a rough approximation to determine points on the phase diagram, and use these to construct a qualitative ‘phase diagram’. In sections 4 and 5 we discuss the two different ensembles, and discuss the effect of varying both temperature and force. In section 6 we introduce a fugacity associated with the number of bends in the polymer, and discover the new phenomenon of a saw-tooth like behaviour in the force-extension curves at sufficiently low temperatures. A brief summary and discussion completes the paper.

2 The model

We model the polymer chains as interacting self-avoiding walks (ISAWs) on the square lattice [20] as shown in Fig. 1. Interactions are introduced between non-bonded nearest neighbor monomers. In our model one end of the polymer is attached to an impenetrable neutral surface (there are no interactions with this surface) while the polymer is being pulled from the other end with a force acting along the x -axis. Note that the ISAW does not extend beyond either end-point so the x -coordinate x_j of the j 'th monomer is restricted by $0 = x_0 \leq x_j \leq x_N = x$. At first this restriction may appear artificial but it does in fact model the experimental setup. In typical experiments single proteins or small pieces of DNA are attached to the surface of beads (using ligand molecules). The beads are very large compared to the size of the proteins and the surface of the bead is thus well approximated by a flat surface.

We introduce Boltzmann weights $\omega = \exp(-\epsilon/k_B T)$ and $u = \exp(-F/k_B T)$ conjugate to the

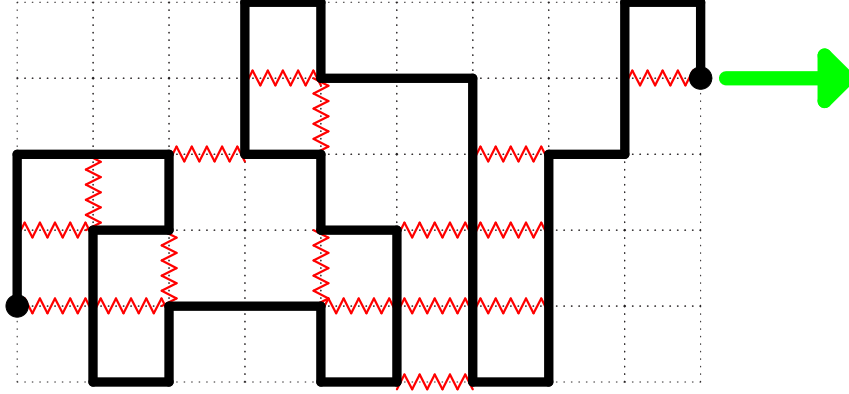


Figure 1: An ISAW on the square lattice with one end attached to a surface and subject to a pulling force on the other end. Monomers are located on the vertices of the lattice and bonds are indicated by the thick solid line. Interactions also occur between non-bonded nearest neighbours as indicated by the zig-zag lines.

nearest neighbor interactions and force, respectively, where ϵ is the interaction energy, k_B is Boltzmann's constant, T the temperature and F the applied force. In the rest of this study we set $\epsilon = -1$ and $k_B = 1$. We study the finite-length partition functions

$$Z_N(F, T) = \sum_{\text{all walks}} \omega^m u^x = \sum_{m, x} C(N, m, x) \omega^m u^x, \quad (1)$$

where $C(N, m, x)$ is the number of ISAWs of length N having m nearest neighbor contacts and whose end-points are a distance $x = x_N - x_0$ apart. The partition functions of the **CFE**, $Z_N(F, T)$, and **CDE**, $Z_N(x, T) = \sum_m C(N, m, x) \omega^m$, are related by $Z_N(F, T) = \sum_x Z_N(x, T) u^x$. The free energies are evaluated from the partition functions

$$G(x) = -T \log Z_N(x) \quad \text{and} \quad G(F) = -T \log Z_N(F). \quad (2)$$

Here $\langle x \rangle = \frac{\partial G(F)}{\partial F}$ and $\langle F \rangle = \frac{\partial G(x)}{\partial x}$ are the control parameters of the **CFE** and **CDE**, respectively.

We enumerate all possible conformations of the ISAW by exact enumeration techniques. The major advantage of this approach is that the complete finite-length partition functions can be analyzed exactly. Furthermore scaling corrections can be taken into account by suitable extrapolation schemes enabling us to obtain accurate estimates in the thermodynamic (infinite length) limit [21].

To achieve a similar degree of accuracy using Monte Carlo simulations one typically has to use chains at least two orders of magnitude longer than in the exact enumerations [22]. The greatest challenge facing exact enumerations is to increase the chain length. Until now most exact results for models of small proteins were confined to chain lengths of 30 or so [23, 24]. Here the number of ISAWs was calculated using transfer matrix techniques [25]. Combined with parallel processing, we were able to almost double the chain length. To be precise we calculate the partition functions up to chain length 55.

3 Fluctuation curves and phase diagram

At low temperature and force the polymer chain is in the collapsed state and as the temperature is increased (at fixed force) the polymer chain undergoes a phase transition to an extended state. The value of the transition temperature (for a fixed value of the force) can be obtained from the fluctuations in the number of non-bonded nearest neighbor contacts (which we can calculate exactly for any finite N up to 55). The fluctuations are defined as $\chi = \langle m^2 \rangle - \langle m \rangle^2$, with the k 'th moment given by

$$\langle m^k \rangle = \frac{\sum_{m,x} m^k C(N, m, x) \omega^m u^x}{\sum_{m,x} C(N, m, x) \omega^m u^x}.$$

In the panels of Fig. 2 we show the emergence of peaks in the fluctuation curves with increasing N at fixed force $F = 0.0$ and $F = 0.5$. In the top right panel we show the growth in the peak value as N is increased. Since this is a log-log plot we see that the peak values grows as a power-law with increasing N ; this divergence is the hall-mark of a phase transition. In the lower right panel we have plotted the position of the peak (or transition temperature) as a functions of $1/N$. Clearly the transition temperature appears to converge to a finite (non-zero) value but the data exhibits clear curvature which makes an interpolation to infinite length difficult.

One can also study the same transition phenomenon by fixing the temperature and varying the force. In the panels of Fig. 3 we show the emergence of peaks in the fluctuation curves with increasing N at fixed temperature $T = 1.0$ and $T = 0.5$. Again we observe the power-law divergence of the peak-value. The only other note-worthy feature is that in the plots of the peak position (critical force value) we observe not only strong curvature but we actually see a turning point in

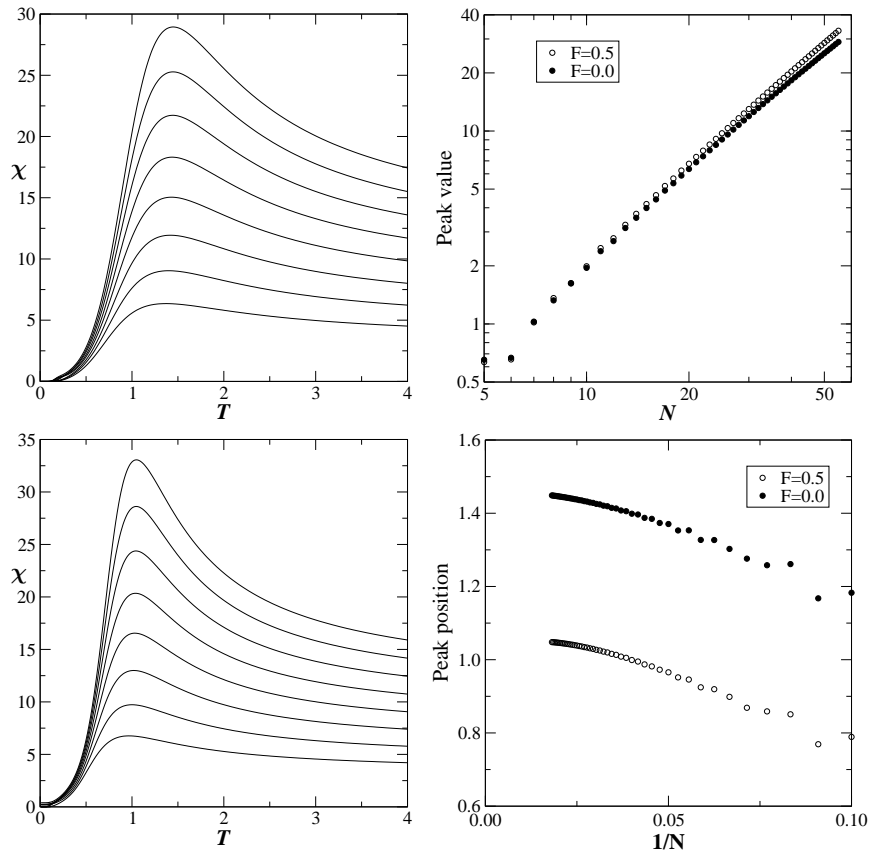


Figure 2: The fluctuations in the number of contacts as a function of temperature for fixed force $F = 0.0$ (upper left panel) and $F = 0.5$ (lower left panel). Each panel contains curves for ISAWs of length (from bottom to top) $N = 20, 25, \dots, 55$. In the upper right panel we show a log-log plot of the growth in the peak value of the fluctuation curve with chain length N . The lower right panel shows the peak position (critical temperature value) vs $1/N$.

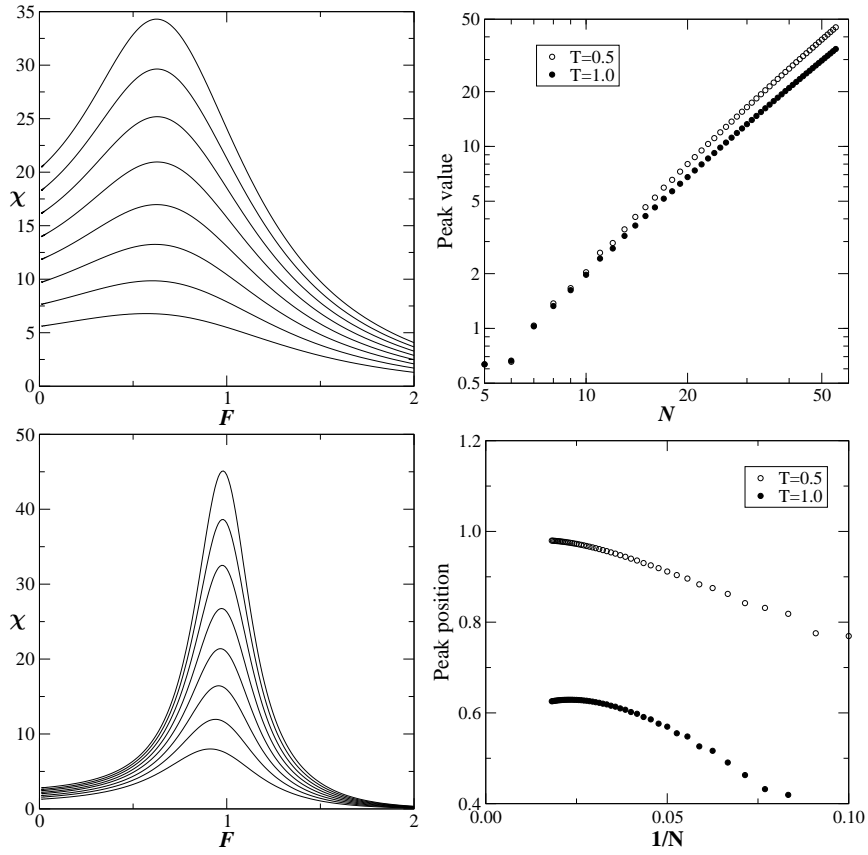


Figure 3: The fluctuations in the number of contacts as a function of force for fixed temperature $T = 1.0$ (upper left panel) and $T = 0.5$ (lower left panel). Each panel contains curves for ISAWs of length (from bottom to top) $N = 20, 25, \dots, 55$. In the upper right panel we show a log-log plot of the growth in the peak value of the fluctuation curve with chain length N . The lower right panel shows the peak position (critical force value) vs $1/N$.

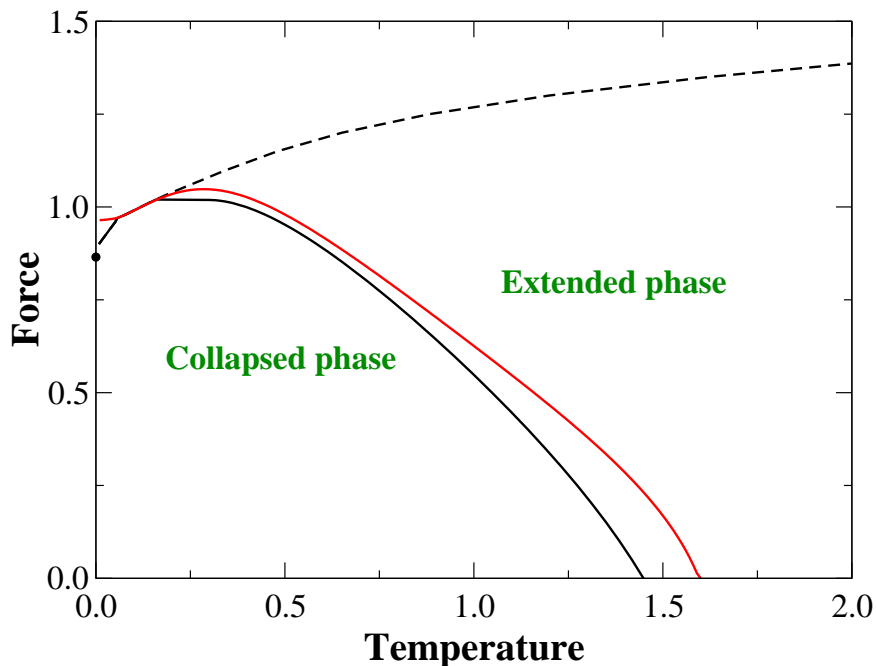


Figure 4: The ‘phase diagram’ for flexible chains as obtained from the position of the peak in the contact fluctuation curves for $N = 55$. The solid black curve and the dashed curve are obtained by fixing the force and varying the temperature. The solid red curve is obtained by fixing the temperature and varying the force.

the curves as N is increased. This feature would make it impossible (given the currently available chain lengths) to extrapolate this data.

In Fig. 4, we show the force-temperature ‘phase diagram’ for flexible chains as obtained from the peak positions (note that the true phase diagram should be obtained by extrapolating our data to the $N \rightarrow \infty$ limit). The qualitative features of the phase diagram remains largely the same as those observed in previous studies [24]. In Fig. 4 we have shown the transitions as obtained by fixing the force (black curves) or fixing the temperature (red curve). One of the most notable feature of the phase-diagram is the *re-entrant* behaviour which can be explained by a ground state with non-zero entropy [24, 26]. Using phenomenological arguments at $T = 0$, the critical force $F_c = 0.8651$ (indicated by a black circle on the y -axis) is found from the expression, $F_c = 1 - 1/\sqrt{N} + TS$ [24]. The positive slope dF_c/dT at $T = 0$ confirms the existence of re-entrance in the $F - T$ phase-diagram. In the panels of Fig. 5 we show the emergence of two peaks in the fluctuation curves with

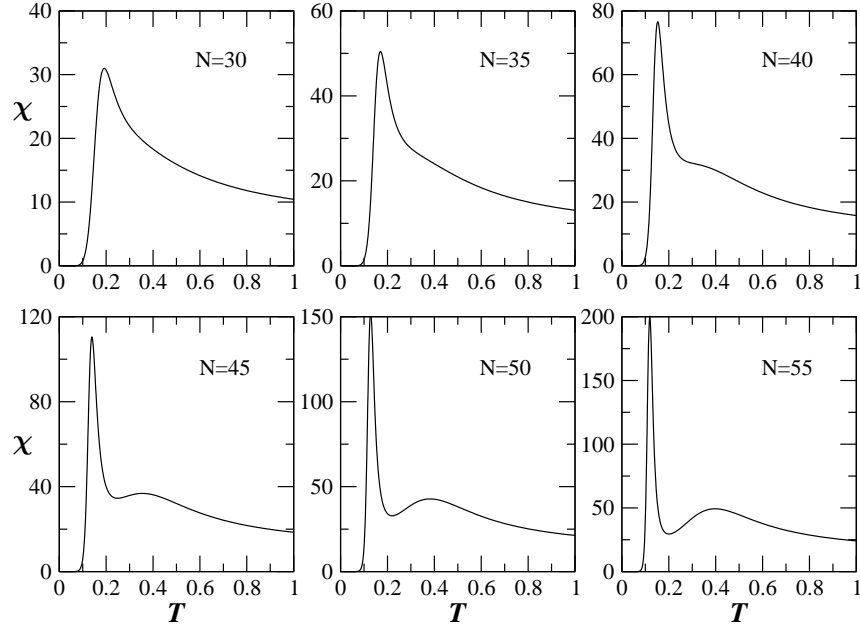


Figure 5: The fluctuations in the number of contacts as a function of temperature for fixed force $F = 1.0$.

increasing N at fixed force $F = 1.0$. The twin-peaks reflect the fact that in the re-entrant region as we increase T (with F fixed) the polymer chain undergoes two phase transitions. Note that the twin-peaks are not apparent for small values of N .

The other notable feature is that in the fixed force case we see a new transition line from the extended state to the fully stretched state which is solely induced by the applied force (the dashed line in Fig. 4. In contrast to the lower phase boundary (collapse transition), where the force decreases with temperature, the upper phase boundary (stretching transition) shows that the force increases with the temperature. However, very curiously, we *do not* observe this upper transition line when we fix the temperature and let the force vary. Indeed this is clear from Fig. 3 where at fixed $T = 0.5$ and 1.0 we see only a single peak (giving us points on the red curve in the phase diagram Fig. 4). In Fig. 3 the value of the force extends up to $F = 2.0$ and the upper transition (dashed line in the phase diagram) should appear (if present) as a second peak in the fluctuation curves of Fig. 3. The absence of any evidence of a second peak is what leads us conclude that we do not see this second transition in the fixed T varying F study. We are not sure whether the

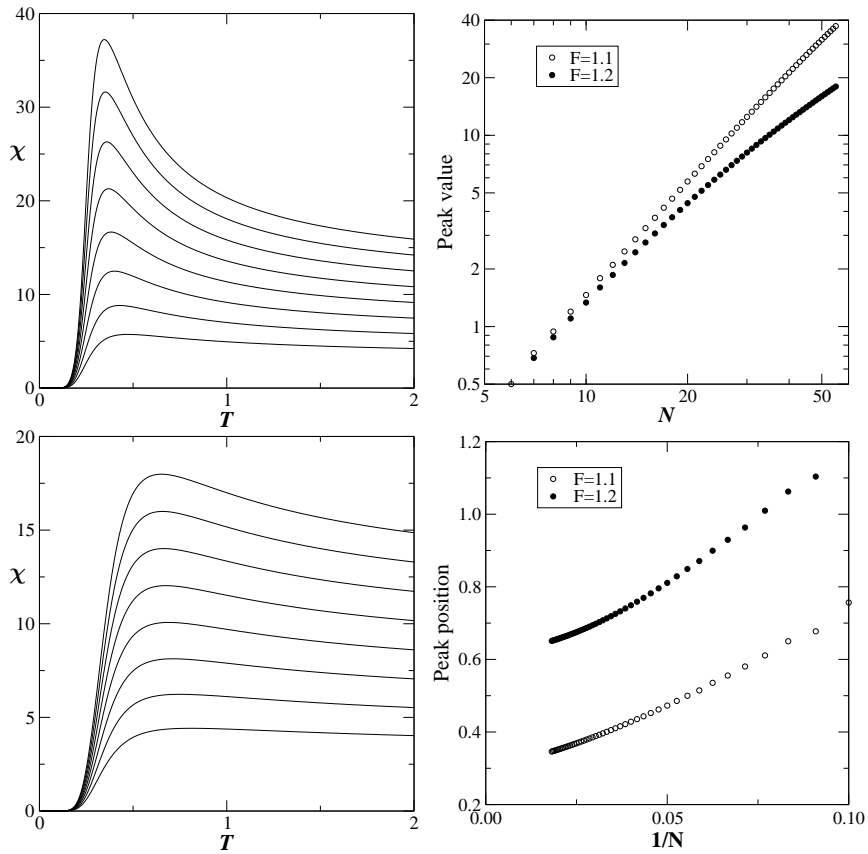


Figure 6: The fluctuations in the number of contacts as a function of temperature for fixed force $F = 1.1$ (upper left panel) and $F = 1.2$ (lower left panel). Each panel contains curves for ISAWs of length (from bottom to top) $N = 20, 25, \dots, 55$. In the upper right panel we show a log-log plot of the growth in the peak value of the fluctuation curve with chain length N . The lower right panel shows the peak position (critical temperature value) vs $1/N$.

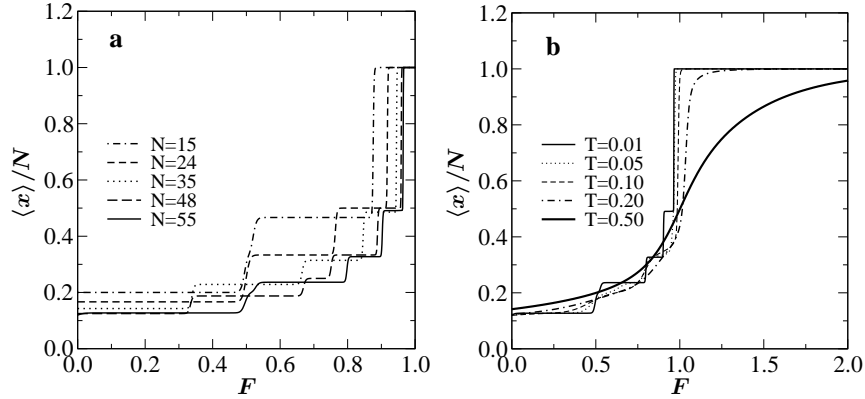


Figure 7: The average scaled elongation $\langle x \rangle / N$ vs F at $T = 0.01$ for various lengths (a) and temperatures at length $N = 55$ (b).

upper phase boundary is a real phase transition or a crossover phenomenon. If it is a real phase transition then the phase-diagram does not really exhibit re-entrance. In re-entrance we go from phase A to phase B and then again to phase A. In Fig. 6 we have plotted the fluctuation curves for force $F = 1.1$ and $F = 1.2$. The curves for $F = 1.1$ (including the plot of the peak height) looks very similar to the plots (see Fig. 3) for low values of the force. For force $F = 1.2$ the peak is not very pronounced and we are hesitant to even call it a peak. Also when we look at the peak height vs. N it appears that the curve has two different behaviours for small and large N , respectively. This could be a sign of a cross-over behaviour. We are currently performing more studies to try to understand and resolve this discrepancy.

4 The constant force ensemble

First we study the model in the **CFE**. In Fig. 7a, we plot the average scaled elongation,

$$\langle x \rangle / N = \frac{1}{N} \frac{\sum_{m,x} x C(N, m, x) \omega^m u^x}{\sum_{m,x} C(N, m, x) \omega^m u^x},$$

as a function of the applied force for different chain lengths at low temperature. Experimentally several transitions were found in the force-extension curves corresponding to many intermediate states [9, 11, 12, 27]. This phenomenon is clearly confirmed by our study. It has been argued that in the limit of infinite chain length, the intermediate states should vanish and there will be an

abrupt transition between a folded and fully extended state [23]. Evidence to this effect can also be seen in Fig. 7a where we note that the plateaus at an extension around 0.2 tends to increase with N while the other plateaus tend to shrink with N (this is particularly so for the plateau around 0.5 corresponding to a simple zig-zag pattern of the chain). Note however, that as we change the chain length from 25 to 55, we find more and more of these intermediate states. This has also been observed in recent experiments [9, 27] where the globule deforms into an ellipse and then into a cylinder. At a critical extension the polymer undergoes a sharp first order transition into a “ball string” conformation [9, 27]. This shows that finite size effects are crucial in all the single molecule experiments and can be seen even for long chains [12].

A simple theoretical argument for the observed behavior is that at low temperature, where the entropy S (per monomer) of the chain is quite low, the dominant contribution to the free energy

$$G = N\epsilon - \sigma(N, F)\epsilon - NTS \quad (3)$$

is the non-bonded nearest-neighbor interaction $N\epsilon$. The second term is a surface correction and it vanishes in the thermodynamic limit. However for finite N , the system has many degenerate states depending upon the shape of the globule. This leads to a surface correction term $\sigma(N, F)$ which is a function of N and F . If $F = 0$ the shape of the globule is like a square and the surface correction term $\sigma(N, 0)$ will be minimized and equal to $2\sqrt{N}$. In the **CFE**, there is a force induced additional contribution proportional to the extension of the globule which along with $\sigma(N, F)$ stabilizes the intermediate states. When the temperature increases the multi-step character of the force-extension curve is washed out due to increased contributions from entropy. This effect can be clearly seen in Fig. 7b where we have plotted force-extension curves at different T .

In the limit $T \rightarrow 0$, and for any fixed N , we can make the argument more precise, and deduce the exact values of the elongation at the plateaus, and the exact values of the force at the transition between two plateaus. Consider for instance the case $N = 55$, cf. Fig. 7a. Our task is to find the conformations that minimize the energy, i.e., maximize the quantity $Fx + m$. For $F \rightarrow 0$ this means just maximizing m , and this is achieved by zigzag conformations inscribed in a rectangle which is as close to a square as possible. The best choice (unique up to trivial lattice symmetries) is the $x \times y = 7 \times 6$ rectangle shown in Fig. 8a, which has $m = 42$, and is responsible for the plateau at

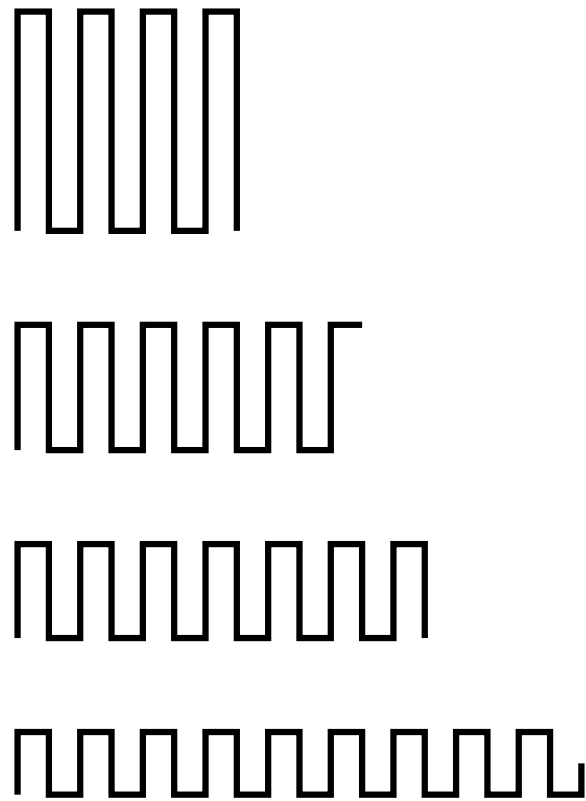


Figure 8: Conformations responsible for the plateaus in the force-elongation curve with $T \rightarrow 0$ and $N = 55$.

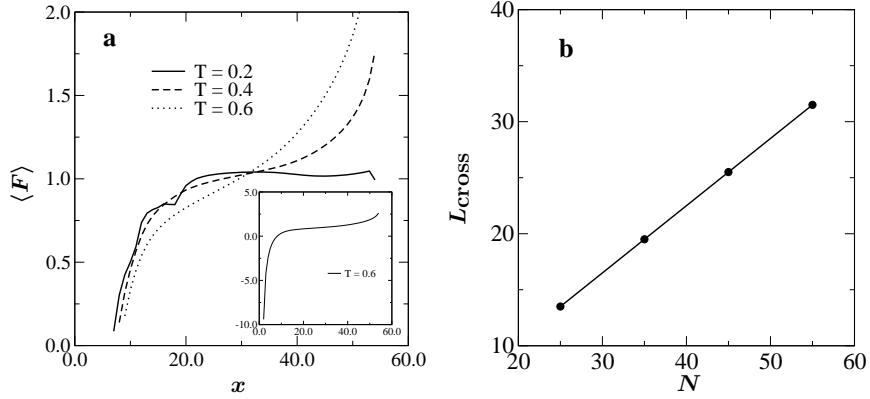


Figure 9: Plot of the average force $\langle F \rangle$ vs the elongation x at various temperatures T for $N = 55$ (a) and the cross-over length vs N (b).

$\frac{x}{N} = \frac{7}{55} \simeq 0.127$. From this conformation it is easy to find other with $m \rightarrow m - 1$ and $x \rightarrow x + 1$ by unzipping a monomer at the boundary, but this is not favorable for $F < 1$. However, at $F = \frac{1}{2}$ the 11×4 conformation of Fig. 8b with $m = 40$, and the 13×3 conformation of Fig. 8c with $m = 39$ start participating. The former is responsible for the shoulder at $\frac{x}{N} = \frac{11}{55} = 0.200$, clearly visible in Fig. 7a. However, the latter becomes the ground state for $F > \frac{1}{2}$, and so the next plateau is at $\frac{x}{N} = \frac{13}{55} \simeq 0.236$. Finally, the 18×2 conformation of Fig. 8d with $m = 35$ starts dominating at $F = \frac{4}{5}$ and is responsible for the plateau at $\frac{x}{N} = \frac{18}{55} \simeq 0.327$.

It is thus evident that the precise plateau structure is extremely dependent on the value of N and the details of the model (e.g., the choice of lattice). However, the following intuitive picture is of a more general validity: The dominant conformation for $F = 0$ fills out a square, and as F is increased more elongated rectangular conformations start dominating. Each of the plateau transitions corresponds to making the rectangle one or a few units thinner in the y direction. In the large N limit, a direct comparison of the conformations with $y = \sqrt{N}$ and $y = \sqrt{N} - 1$ shows that indeed the first plateau will dominate for all $F \in [0, 1)$, as expected from an inspection of Fig. 7a, and in agreement with Ref. [23].

5 The constant distance ensemble

Next we study the model in the **CDE**. The force-extension curve shown in the insert of Fig. 9a has interesting features. It shows that when the distance between the first and the last monomer (where force is applied) is less than the average size of the coil (without force), one needs a compressing force instead of a pulling force. The qualitative behavior is similar to one observed in experiments [28] and computer simulations [29]. Since most models do not include confinement in their description, such behavior could not be predicted. In Fig. 9a, we show the response of the force when the elongation exceeds the average size of the polymer. The flat portion of the curve gives the average force needed to unfold the chain. Such plateaus have been seen in experiments [9, 12, 11]. From Fig. 9a one can also see that the force required to obtain a given extension initially decreases with temperature. But beyond a certain extension (close to 30 in this case) the required force increases with temperature. We note that the curves cross each other at a ‘critical’ extension for any temperature (below the θ -point). We identify this as a cross-over point. In Fig. 9b we plot the position of the cross-over point L_{cross} as a function of the length N of the polymer chain. We see that the crossover extension increases linearly with the chain length. This shows that above this point the chain acquires the conformation of the stretched state. The increase in force with temperature generates a tension in the chain sufficient to overcome the entropic effect. Since the contribution to the free energy from this term is TS (S being the entropy), more force is needed at higher T as seen in experiments. Our exact analysis for finite chain length shows that applying a force at first favors taking the polymer from the folded state to the unfolded state. However, rupture or second unfolding occurs when the tethered or unfolded chain attains the stretched state, and one requires more force at higher temperature.

6 Semi-flexible polymers

We model semi-flexible polymers by associating a positive energy ϵ_b with each turn or bend of the walk [24]. The corresponding Boltzmann weight is $\omega_b = \exp(-b\epsilon_b)$, where b is the number of bends in the ISAW. We again enumerate all walks, but because of the additional parameter ω_b ,

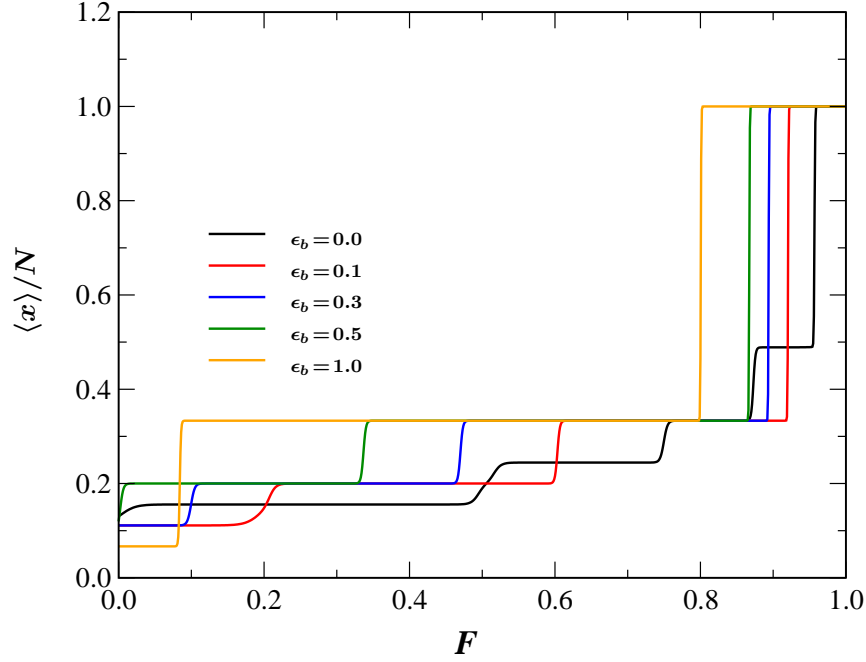


Figure 10: Plot of the average scaled elongation $\langle x \rangle / N$ vs F for semi-flexible chains with bending energy ranging from $\epsilon_b = 0.0$ (flexible chains) to $\epsilon_b = 1.0$ at low temperature $T = 0.01$ for chain length $N = 45$

we were restricted to 45 steps. For a semi-flexible polymer chain, a stretched state may be favored by increasing the stiffness. The phase diagram for semi-flexible chains is now well established. It has three states namely (i) an open coil state at high temperature, (ii) a molten globule at low temperature and low stiffness and (iii) a 'frozen' or 'folded' state at low temperature and large stiffness [17, 18, 24]. We note that while the flexible and semi-flexible $F - T$ phase-diagrams are qualitatively similar [24], the re-entrant behavior is suppressed because of stiffness and becomes less pronounced with increasing bending energy.

In Fig. 10, we plot the force-extension curves for semi-flexible chains with bending energy ranging from $\epsilon_b = 0.0$ (fully flexible chains) to $\epsilon_b = 1.0$ at low temperature $T = 0.01$ for chain length $N = 45$. We observe that as the bending energy is increased the chain undergoes fewer intermediate transitions between the compact state (low force) and the fully stretched state (high force). In particular the flexible chain ($\epsilon_b = 0.0$) has five plateaus while the chain with $\epsilon_b = 1.0$ has only three. This can again be explained more quantitatively by inspecting the dominant

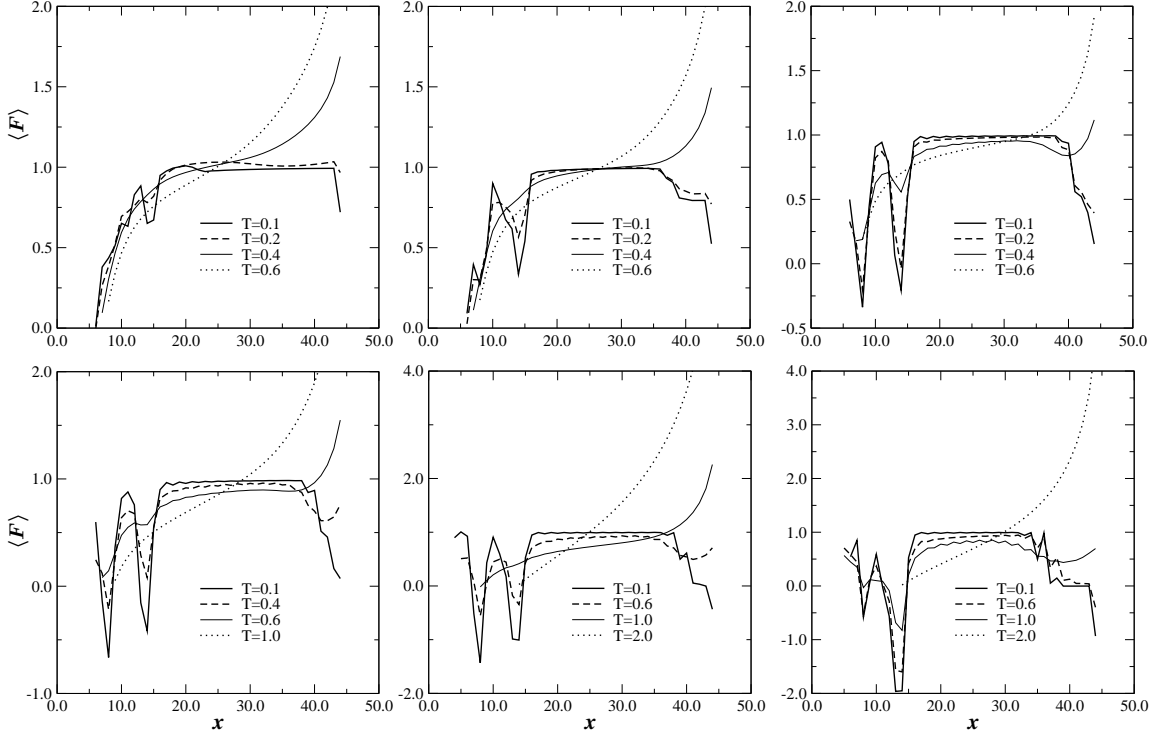


Figure 11: Plot of $\langle F \rangle$ vs x for a semi-flexible chain with bending energy (from left to right and top to bottom) $\epsilon_b = 0.0, 0.1, 0.3, 0.5, 1.0$ and 2.0 at different temperatures T for $N = 45$

configurations in the limit $T \rightarrow 0$, as in section 4 above.

In the **CFE**, the probability distribution of the end-to-end distance has "saw-tooth" like behavior corresponding to intermediate states during unfolding [24]. Therefore, it is important to study the effect of stiffness on force-extension curves in the **CDE**. The force extension curves shown in Fig. 11 have striking differences from the flexible ones. At low temperatures we see strong oscillations which vanish as the temperature is increased. As the bending energy is increased and the polymer becomes more rigid the oscillatory behavior extends to higher and higher temperatures. Since the polymer chain has "frozen conformations" like β -sheets (the zero-force limit of which describes zig-zag configurations inscribed in a square), it takes more force to unfold a layer. When about half a layer has been opened, the bending energy favors a complete stretching of the layers and hence the force decreases. This phenomenon allows us to probe a molecule like Titin which has similar β -sheet structure [30].

7 Summary and discussion

To summarize, we have presented the exact solution of a model of long (finite) polymer chains, of direct relevance to recent experiments on the elastic properties of single biomolecules. The model takes into account several constraints imposed by the experimental setups: geometric constraints, excluded volume effects, attraction between chain segments, finite but large chain length (here up to $N = 55$). It permits one to choose the thermodynamic ensemble (**CFE** or **CDE**) dictated by the experimental protocol. The exact enumeration data permits us to access all parameter values, including biologically relevant low temperatures where previous studies have failed. Our results correctly reproduce several experimentally observed effects: multiple transitions during unfolding, “saw-tooth” like oscillations in the force-extension curve of semi-flexible chains and first-order transition into a “ball string” conformation. Finally, we have identified cross-over behavior that provides a unified treatment of both pulling and compressing forces in the **CDE**.

Acknowledgments

We would like to thank the Australian Research Council (IJ,AJG), the Indo-French Centre for the Promotion of Advanced Research (CEFIPRA) (JLJ) and MPIPKS, Dresden, Germany (SK). The calculations presented in this paper used the computational resources of the Australian Partnership for Advanced Computing (APAC) and the Victorian Partnership for Advanced Computing (VPAC).

References

- [1] M. Rief *et al*, *Science* **276** (1997) 1109.
- [2] M. S. Z. Kellermayer *et al*, *Science* **276** (1997) 1112; L. Tskhovrebova *et al*, *Nature* **387** (1997) 308.
- [3] C. Bustamante *et al*, *Annu. Rev. Biochem.* **73** (2004) 705.
- [4] L. S. Itzhaki and P. A. Evans, *Protein Sci.* **5**, (1996) 140.
- [5] I. Rouzina and V. A. Bloomfield, *Biophys. J.* **80** (2001) 882; *ibid* **80** (2001) 894.

- [6] E. Evans and K. Ritchie, *Biophys. J.* **72** (1997) 1541; *ibid* **76** (1999) 2439.
- [7] S. M. Bhattacharjee, *J. Phys. A* **33** (2000) L423.
- [8] C. Bustamante, Z. Bryant, and S. B. Smith, *Nature* **421** (2003) 423.
- [9] B. J. Haupt, T. J. Senden, and E. M. Sevick, *Langmuir* **18** (2002) 2174.
- [10] P. G. de Gennes *Scaling Concepts in Polymer Physics* (Cornell University Press: Ithaca, 1979).
- [11] H. Mao *et al* , *Biophys. J.* **89** (2005) 1308.
- [12] A. S. Lemak, J. R. Lepock, and J. Z. Y. Chen, *Phys. Rev. E* **67** (2003) 031910; *Proteins: Structures, Function and Genetics* **51** (2003) 224.
- [13] C. Bustamante, J. Liphardt, and F. Ritort, *Phys. Today* **58** (2005) 43.
- [14] M. Zemanova and T. Bleha, *Macromol. Theory Simul.* **14** (2005) 596.
- [15] M. Fixman, *J. Chem. Phys.* **58** (1973) 1559.
- [16] M. Doi and S. F. Edwards, *Theory of Polymer Dynamics* (Oxford University Press: Oxford, 1988).
- [17] U. Bastolla and P. Grassberger, *J. Stat. Phys.* **89** (1997) 1061.
- [18] S. Doniach, T. Garel. and H. Orland, *J. Chem. Phys.* **105** (1996) 1601.
- [19] S. Kumar *et al*, *Phys. Rev. Lett.* **98** (2007) 128101.
- [20] C. Vanderzande, *Lattice Models of Polymers* (Cambridge University Press: Cambridge, 1998).
- [21] A. J. Guttmann, *Phase Transitions and Critical Phenomena* vol. 13, edited by C. Domb and J. L. Lebowitz (Academic Press: New York, 1989).
- [22] Y. Singh, D. Giri, and S. Kumar, *J. Phys. A* **34** (2001) L67.
- [23] D. Marenduzzo *et al*, *Phys. Rev. Lett.* **90** (2003) 088301.
- [24] S. Kumar and D. Giri, *Phys. Rev. E* **72** (2005) 052901; *Phys. Rev. Lett.* **98** (2007) 048101.

- [25] I. Jensen, *J. Phys. A* **37** (2004) 5503.
- [26] E. Orlandini *et al*, *J. Phys. A* **34** (2001) L751; D. Marenduzzo *et al*, *Phys. Rev. Lett.* **88** (2002) 028102.
- [27] H. Dietz and M. Rief (2004) *PNAS* **101** (2004) 16192.
- [28] M. C. Guffond, D. R. M. Williams, and E. M. Sevick, *Langmuir* **13** (1997) 5691.
- [29] J. Jimenez and R. Rajagopalan, *Langmuir* **14** (1998) 2598.
- [30] M. Rief *et al*, *Science* **275** (1997) 1295.